J Electroceram (2009) 23:62–66
DOI 10.1007/s10832-008-9535-x

ZnO-based varistor thick films with high non-linear electrical behavior

Marco Peiteado · Miguel Angel De la Rubia · José De Frutos · Teresa Jardiel

Received: 5 February 2008 / Accepted: 26 June 2008 / Published online: 10 July 2008

Abstract Thick films of ZnO-based ceramic varistors prepared by tape casting technique typically show a poor electrical response that still limits their application as protective devices. The excessive volatilization of Bi_2O_3 during sintering at high temperatures, especially dramatic in the film geometry due to its high area–volume ratio, is found to be the origin of this poor electrical behavior. The problem is overcome by sintering the films in a controlled Bi-rich sealed atmosphere, leading to a high reliability and reproducibility in their non-linear response.

Keywords Varistor · ZnO · Thick films · Bismuth vaporization · Electrical properties

1 Introduction

Bismuth-doped zinc oxide based ceramics with extensive nonlinear current-voltage characteristics are widely used as protective components against transient over-voltages [1–5]. In doing so, these variable resistors, mostly known as varistors, found application in different electric circuits, from electronic devices to power transmission lines. However to meet the requirement of repeatedly withstand high power pulses (large energy-handling capabilities) their use is mostly restricted to bulk specimens. Recently, the potential of thick films for low voltage electrical circuits have attracted attention [6–8], with those manufactured by tape casting and screen printing techniques being the most promising ones. Both technologies have been developed in the field of microelectronics and among their many advantages, the low cost, the possibility of miniaturization and the design versatility can be enumerated. Nevertheless some critical technological problems still are unsolved. Particularly in the case of varistor thick-films a lack of reproducibility in the electrical response is still obtained that specially limits their functionality as protective devices. In addition the maximum non-linearity that could be achieved is about $\alpha \sim 20$ [9]. This value is still far from the electrical response obtained in bulk ceramics, typically with $\alpha \geq 40$. The origin of this poor varistor behavior in thick film geometry should be found on an excessive bismuth loss by vaporization during the sintering of the ceramic [10, 11]. This volatilization takes place from the Bi-rich liquid phase formed in the system. Bismuth is added to the varistor formulation to promote the formation of the Double Schottky Barriers at grain boundaries (varistor forming dopant) [12–14]: a very thin layer of segregated Bi is placed between ZnO grains inducing electronic interface states that can trap charges, so electrostatic potential barriers are built up at these grain boundaries given place to the non-linear behavior [1, 15–17]. Additionally, bismuth oxide forms a liquid phase on sintering which favors the densification process of the ceramic. So in this sense the volatilization of bismuth has dramatic consequences on the varistor microstructure as well as on

M. Peiteado (✉)
Department of Electroceramics,
Instituto de Cerámica y Vidrio (CSIC),
Kelsen 5,
28049 Madrid, Spain
e-mail: mpeiteado@icv.csic.es

M. A. De la Rubia · J. De Frutos
Applied Physics Department, E.T.S.I. Telecomunicación (UPM),
28040 Madrid, Spain

T. Jardiel
Materials Science and Engineering Department,
Universidad Carlos III de Madrid,
28911 Leganés, Spain

its electrical response. But moreover, in previous works with bulk varistor samples we found that bismuth volatilization increases noticeably not only with the sintering temperature, but also with the area–volume ratio of the ceramic compact [18]. Such effect is obviously more accentuated in the thick film geometry, where the area–volume ratio is about two orders of magnitude higher than in bulk samples. To minimize these losses a decrease of the sintering temperature could be attractive. However this is not a realistic solution since high sintering temperatures are manifestly required to build up the defect structure of potential barriers at grain boundaries that leads to a high non-linear response. In other words, to prepare varistor thick films for protective applications two confronted parameters have to be faced: on the one hand high sintering temperatures have to be applied but on the other hand these high temperatures will promote the vaporization of Bi with the consequent deterioration of the film electrical response. In the present contribution we solve this problem by sintering the films in a controlled Bi-rich atmosphere. This will avoid a massive vaporization of Bi at high temperatures, even for high area–volume ratio geometries. As a consequence an elevated and reproducible non-linear response is observed in the prepared films.

2 Experimental procedure

2.1 Preparation of the films

A standard varistor composition comprising ZnO (95.5 mol%), Bi_2O_3 (0.5), Sb_2O_3 (1.5), Co_3O_4 (0.5), MnO (0.5), NiO (1) and SnO_2 (0.5) was used. The powder was obtained by means of a classical mixed-oxide route including ball milling for 2 h in ethanol. After that, the powder was calcined at 950°C–1 h and again milled. This calcination strategy has been previously applied successfully to obtain a high degree of microstructural homogeneity in the ceramic [19].

The paste was prepared by mixing the varistor powder (60 wt.%) with an organic vehicle (40 wt.%) that provides flexibility as well as good homogeneity, in a planetary mill. The organic vehicle is composed of a mixture of ethanol and methyl ethyl ketone as solvent, polyvinyl buthyral as binder and polyethylene glycol and benzyl buthyl ftalate as plasticizers [20]. Rheological characterization of the varistor paste showed a pseudoplastic behavior with a viscosity value of $\eta \sim 4{,}500$ mPas for a shear rate of 200 s^{-1}. Thick films were prepared by casting the slurry over a polymer sheet which is easily removed after drying the film at room temperature. Once the sheets were removed, the films were deposited onto a high purity dense alumina substrate. This substrate was previously covered with a platinum electrode ink (DuPont 4191) by screen printing; moreover, to provide a strong adhesion between the electrode and the substrate, the Pt/Al_2O_3 substrate couple was fired at 850°C for 30 min. The whole assembly, film–Pt–substrate, was then subjected to a hot press step at 80°C/0.6 bar for 10 min to stick the films onto the substrates. Following that, a heat treatment at 500°C for 2 h, with a heating rate of 0.2°C/min and a cooling rate of 1°C/min [20], was applied to remove the organic vehicle of the film. This heat treatment gave place to green thicknesses around 60–70 μm. The assembly was finally sintered at 1150°C for 1 h and thick films of 30–35 μm thickness were obtained. However in order to obtain a reliable electrical response, the microstructure of the sintered material should contain a meaningful number of grains between the electrodes. If we assume an average ZnO grain size of 8 to 10 microns (typical for bulk specimens sintered above 1100°C [1]), the final thickness of the sintered films should be around 100 μm. According to this the whole processing was performed as described, but this time staking three of the casted films together; after sintering a final average thickness around 100 μm was obtained. To control the excessive volatilization of Bi_2O_3, the sintering was carried out in a Bi-rich atmosphere. Such atmosphere was achieved by preparing the following assemblage: the films were enclosed by placing face down one dense alumina crucible internally sealed with Bi_2O_3 powder (see chart in Fig. 1). This will provide the mandatory Bi rich atmosphere for sintering the films. In addition the crucible was outside sealed with spinel phase powder to minimize the losses of the extra Bi_2O_3 from the internal sealing (b.p. ~ 830°C). By reacting with the spinel powder the Bi_2O_3 will form pyrochlore, so diffusion across the crucible joint will be prevented.

For comparison varistor thick films were also sintered at 1150°C for 1 h in open air. Also bulk cylindrical pellets (15 mm in height and diameter) of the starting powder were prepared and sintered in air atmosphere at 1200°C for 2 h (optimal sintering conditions for these bulk specimens [21]).

2.2 Samples characterization

Phase characterization of the starting varistor powder was performed by x-ray diffraction (XRD) on a D5000 Siemens

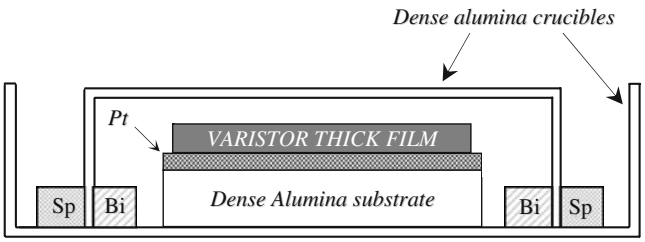

Fig. 1 Assembly for sintering the varistor thick films under Bi-rich atmosphere

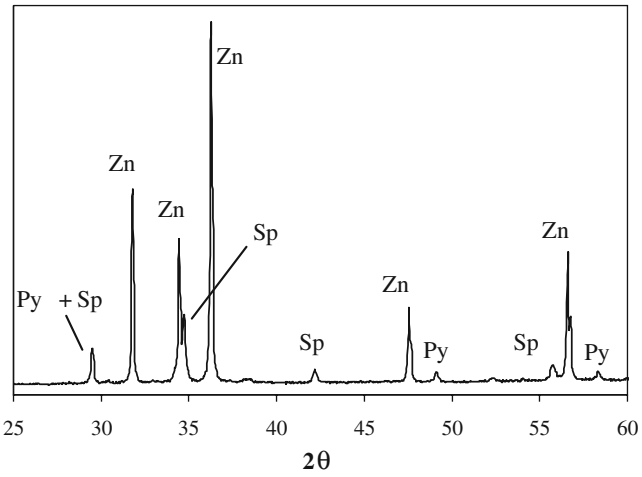

Fig. 2 XRD pattern of the starting varistor powder; Zn = ZnO, Sp = $Zn_7Sb_2O_{12}$ spinel-type phase and Py = $Bi_3Zn_2Sb_3O_{14}$ pyrochlore-type phase

diffractometer using CuKα_1 radiation. Porosity measurements of the green samples were carried out by means of mercury intrusion with a Pore Master equipment of Quantachrome Instruments. This was performed to check that any problem with further densification on sintering could only be related to the Bi volatilization, and not to heterogeneities in the green sample. Green densities in the range 3.1–3.2 g/cm^3 were achieved for both the films and the pellets, meaning ~ 55% of the varistor theoretical density (typically estimated around 5.6–5.7 g/cm^3). For microstructural observations scanning electron microscopy (SEM) was carried out using a cold field emission-scanning electron microscope (model S-4700, Hitachi) equipped with an energy dispersive spectroscopy microanalysis probe (EDS). The distribution of phases and the average ZnO grain size was evaluated from FE-SEM micrographs by an image processing and analysis program (Leyca Qwin); the program measures the surface of each grain and transforms its irregularly shaped area into a circle of equivalent diameter. More than 300 grains were considered for each measurement. Finally for electrical characterization gold electrodes were deposited by sputtering on the top of the film and current density-field strength (J-E) measurements were carried out using a DC power multimeter (Keithley 2410); the value of the non-linearity coefficient α was evaluated from the current density range between 1 and 10 mA/cm^2 using the standard formula [22], the breakdown voltage (or breakdown field strength E_B to make it independent of sample geometry) was measured at 0.3 mA/cm^2 and the leakage current density (J_L) was measured at 85% of E_B.

3 Results and discussion

In a typical varistor composition based on the ZnO–Bi_2O_3–Sb_2O_3 ternary system, the Bi-rich liquid phase is mainly formed together with a $Zn_7Sb_2O_{12}$ spinel-type phase after the decomposition of an intermediate $Bi_3Zn_2Sb_3O_{14}$ pyrochlore-type compound [15, 23]. As previously reported this pyrochlore phase starts to form at temperatures as low as 500°C, i.e., previous to the appearance of the liquid in the microstructure (typically around 740°C, depending on the composition) [24]. In this sense when the composition is formulated with the amount of antimony higher than that of bismuth, mostly all the bismuth will be retained in the pyrochlore structure until its decomposition at high temperature. Figure 2 depicts the XRD pattern of the starting varistor powder after the calcination step at 950°C for 1 h. As observed together with the peaks of the ZnO major phase, peaks of secondary $Bi_3Zn_2Sb_3O_{14}$ pyrochlore-type and $Zn_7Sb_2O_{12}$ spinel-type phases are also detected at this temperature. No traces of free Bi_2O_3 are observed since as mentioned it is mostly trapped in the pyrochlore structure with the corresponding amount of Sb_2O_3 and ZnO. The observed peaks of the spinel phase come from the reaction between the remaining Sb_2O_3 (in excess with regards to Bi_2O_3, Sb/Bi=3), and ZnO. Such reaction is observed to

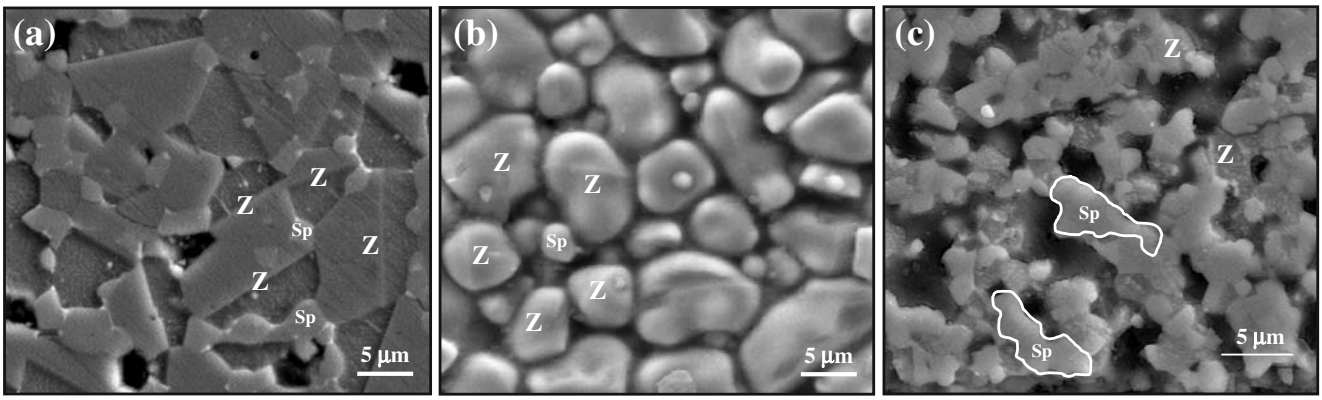

Fig. 3 FE-SEM micrographs corresponding to: (**a**) bulk varistor sample sintered at 1200°C–2 h in air, (**b**) film sintered at 1150°C–1 h in Bi-rich sealed atmosphere, and (**c**) film sintered at 1150°C–1 h in open air. *Z*: ZnO grains, *Sp*: $Zn_7Sb_2O_{12}$ spinel grains

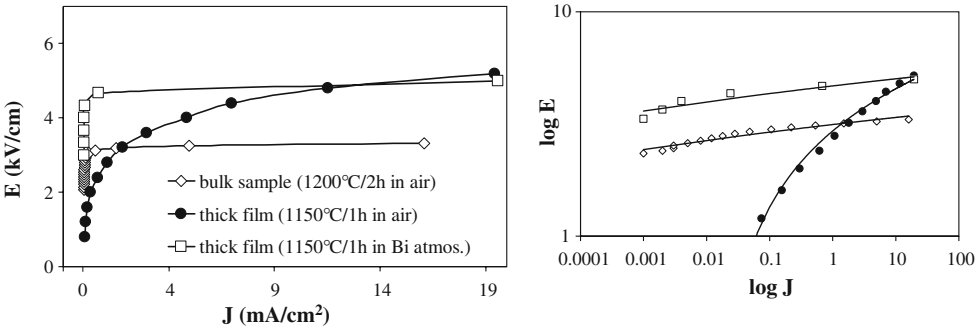

Fig. 4 Current density-field strength (J-E) curves for the thick films and bulk varistor samples prepared in this study. On the *left*, log–log representation for better visibility of the differences in the low current region

take place around 800°C [24]. The presence of the spinel particles prior to the liberation of the liquid is the main reason of the high microstructural homogeneity achieved with this calcination. When the liquid will be released on sintering, these spinel inclusions will exert a pinning effect controlling the ZnO grain growth process.

Figure 3 shows the FE-SEM micrographs of the thick films and bulk samples after the sintering stage. In the case of the bulk varistor sample, the surface of the pellet was previously polished and chemically etched. The films on the other hand were softly etched with acetic acid, in order to avoid the complete removal of the remaining bismuth oxide. As it is observed in Fig. 3(a), the bulk specimen shows a characteristic varistor microstructure comprised by a majority phase of ZnO grains and a secondary phase of $Zn_7Sb_2O_{12}$ spinel grains homogeneously distributed at the triple points between ZnO grains. The volumetric fractions of these phases were estimated from SEM images yielding around 82% for the ZnO grains and 16% for the spinel inclusions. The remaining 2% corresponds to the Bi-rich phase, located at the triple and multiple points (brightest white areas in Fig. 3(a)) and at the ZnO–ZnO grain boundaries. The microstructural analysis revealed a similar distribution of phases for the films sintered under a Bi-rich atmosphere: ZnO grains homogeneously distributed for the whole ceramic, with the smaller spinel grains mostly located at the triple points (Fig. 3(b)). Although the chemical etching has practically removed all the Bi-rich phase, the quantification of the phases yields similar volume fractions for the ZnO and the Zn_7Sb_2O12 spinel grains, 81 and 16% respectively. The only differences between these films and the bulk samples come from the ZnO grain size with an average value of 9.5±0.5 μm for the bulk pellets and of 7.3±0.5 μm in the case of the films (after sintering the average thickness of the thick films was about 100 μm).

But the situation is clearly different in the case of the films sintered in air. A poorly developed microstructure with heterogeneous accumulations of ZnO grains and spinel particles is obtained, as can be seen in Fig. 3(c). Furthermore, a manifest problem of densification is also observed in these films. In addition the average ZnO grain size is below 5 μm, i.e., clearly smaller than that of the pellets or the films sintered under Bi atmosphere. All these microstructural features should be attributed to the elevated bismuth loss by vaporization that takes place in these films sintered in air. As the temperature increases, the special geometry of the films leads to a high Bi volatilization process. As a consequence less liquid phase is available and hence the ceramic hardly densifies, the microstructure is more porous and less homogenous and the ZnO grains grow slower. To corroborate this fact the samples were weighted before and after the sintering step at 1150°C. In doing so, we assume that once the varistor powder is calcined at 950°C, all changes in the mass of the sample are due to the bismuth loss. The results showed no significant weight losses for the film sintered in a Bi-rich atmosphere, whereas a weight loss proportional to almost half of the formulated Bi concentration was obtained for the film sintered in air at this temperature.

These microstructural characteristics should have their corresponding reflection on the electrical properties of the prepared samples. A good electrical response could be expected for the bulk specimens and the films sintered in a Bi-rich atmosphere, whereas a poor behavior could be predicted for the films sintered in open air. The shape of the J-E curves depicted in Fig. 4 confirmed this hypothesis. As observed a quite rounded transition from the region of low currents to the highly conductive state is obtained when the films are sintered in air. This is indicative of a poor non-linearity but also of a high level of leakage current density; this parameter measures the current across the varistor in "standby" (i.e. below the varistor breakdown voltage) and

Table 1 Electrical response of thick films and bulk varistor samples after sintering.

	Thick films sintered in air atmosphere (1150°C/1 h)	Thick films sintered in Bi-rich sealed atmosp. (1150°C/1 h)	Bulk samples sintered in air atmosphere (1200°C/2 h)
α	20	43	55
E_B (kV/cm)	2.0	4.1	2.5
J_L (mA/cm^2)	0.23	0.003	0.011

typically dc current densities above 0.1–0.2 mA/cm^2 are related to unacceptable losses in operating conditions [2]. Such a poor functionality of the films sintered in air is also inferred from the electrical parameters of Table 1. They show a non-linearity coefficient not higher than 20 and an intolerable level of leakage current density for these films. Furthermore a significant degree of data scattering was obtained in these measurements, with around half of the sputtered electrodes leading to erroneous values. Such a lack of reproducibility in the electrical response again evidences a poorly developed microstructure. But once at this point we could also attribute this lack of homogeneity to possible interactions of the varistor film with the Pt electrodes and/or the substrate during the sintering of the assembly. We checked this hypothesis by analyzing the films in the microscope. By means of EDS no diffusion of Bi into the Pt electrode was experimentally detected at the temperature of our test, 1150°C. In the same way we observed that the Pt is confined to the electrode, neither diffusing into the film nor into the dense (sintered) alumina. The fact is that the previous thermal treatment at 850°C of the couple Pt/Al_2O_3 before the deposition of the varistor film (see experimental section), noticeably reduces the possibility of further interactions between the varistor film and the electrode/substrate.

Another evidence for the microstructural influences is that the curves and the electrical parameters of the films sintered in a sealed Bi-rich atmosphere are considerably better, with values of α above 40 and a leakage current density as low as 0.003 mA/cm^2. In addition the electrical response is now very reproducible in these films, with 80–90% of the sputtered electrodes showing the same behavior. Furthermore, Table 1 also shows that the data corresponding to the films sintered in Bi atmosphere are in the same range as those of the bulk samples; the only difference comes from the value of the breakdown field strength, but this is just a consequence of the different ZnO grain size achieved with each processing method.

4 Conclusions

The enormous area–volume ratio of thick film geometry represents a critical parameter for obtaining ZnO-based varistor thick films with high non-linear electrical response due to excessive volatilization of Bi_2O_3 during sintering at high temperatures. These high temperatures are required to build up the defect structure of potential barriers at grain boundaries, which is responsible for the non-linear behavior. The problem is solved by sintering the films under a controlled Bi-rich sealed atmosphere, thereby minimizing the bismuth losses. As a consequence ZnO-based varistor thick films with electrical properties similar to bulk specimens can be obtained. This result is quite innovative and will allow the exploitation of ZnO-based varistor thick films as surge protective devices for low and medium voltage applications.

Acknowledgements This work has been conducted within the CICYT MAT 2007-66845-C02-01 project.

References

1. D.R. Clarke, J. Am. Ceram. Soc **82**, 485 (1999)
2. T.K. Gupta, J. Am. Ceram. Soc **73**, 1817 (1990) doi:10.1111/j.1151-2916.1990.tb05232.x
3. C.M. Barrado, E.R. Leite, P.R. Bueno, E. Longo, J.A. Varela, Mater. Sci. Eng. A **371**, 377 (2004) doi:10.1016/j.msea.2003.09.069
4. Y.W. Lao, S.T. Kuo, W.H. Tuan, J. Electroceram **19**, 187 (2007) doi:10.1007/s10832-007-9187-2
5. M.A. Ramírez, A.Z. Simoes, M.A. Márquez, Y. Maniette, A.A. Cavalheiro, J.A. Varela, Mater. Res. Bull **42**, 1159 (2007) doi:10.1016/j.materresbull.2006.09.001
6. R. Lou-Moeller, C.C. Hindrichsen, L.H. Thamdrup, T. Bove, E. Ringgaard, A.F. Pedersen et al., J. Electroceram **19**, 333 (2007) doi:10.1007/s10832-007-9055-0
7. F. Menil, H. Debeda, C. Lucas, J. Eur. Ceram. Soc **25**, 2105 (2005) doi:10.1016/j.jeurceramsoc.2005.03.017
8. D. Belavic, M. Hrovat, J. Holc, M.S. Zarnik, M. Kosec, M. Pavlin, J. Electroceram **19**, 363 (2007) doi:10.1007/s10832-007-9064-z
9. M.A. De la Rubia, M. Peiteado, J. De Frutos, F. Rubio-Marcos, J.F. Fernández, A.C. Caballero, J. Eur. Ceram. Soc **27**, 3887 (2007) doi:10.1016/j.jeurceramsoc.2007.02.057
10. R. Metz, H. Delalu, J.R. Vignalou, N. Achard, M. Elkhatib, Mater. Chem. Phys **63**, 157 (2000) doi:10.1016/S0254-0584(99)00227-8
11. M. Peiteado, M.A. De la Rubia, M.J. Velasco, F.J. Valle, A.C. Caballero, J. Eur. Ceram. Soc **25**, 1675 (2005) doi:10.1016/j.jeurceramsoc.2004.06.006
12. F. Greuter, Solid State Ion **75**, 67 (1995) doi:10.1016/0167-2738(94)00181-Q
13. C. Leach, Acta Mater **53**, 237 (2005) doi:10.1016/j.actamat.2004.07.006
14. Y. Sato, T. Yamamoto, Y. Ikuhara, J. Am. Ceram. Soc **90**, 337 (2007) doi:10.1111/j.1551-2916.2006.01481.x
15. E. Olsson, G.L. Dunlop, R. Österlund, J. Am. Ceram. Soc **76**, 65 (1993) doi:10.1111/j.1151-2916.1993.tb03690.x
16. A.C. Caballero, D. Hevia, J. De Frutos, M. Peiteado, J.F. Fernández, J. Electroceram **13**, 759 (2004) doi:10.1007/s10832-004-5188-6
17. D. Fernández-Hevia, M. Peiteado, J. De Frutos, A.C. Caballero, J.F. Fernández, J. Eur. Ceram. Soc **24**, 1205 (2004) doi:10.1016/S0955-2219(03)00411-4
18. M.A. De la Rubia, M. Peiteado, J.F. Fernández, A.C. Caballero, J. Eur. Ceram. Soc **24**, 1209 (2004) doi:10.1016/S0955-2219(03)00410-2
19. M.A. De la Rubia, M. Peiteado, J.F. Fernández, A.C. Caballero, J. Holc, S. Drnovsek et al., J. Eur. Ceram. Soc **26**, 2985 (2006) doi:10.1016/j.jeurceramsoc.2006.02.016
20. J.F. Fernández, E. Nieto, C. Moure, P. Durán, R.E. Newnham, J. Mater. Sci **30**, 5399 (1995) doi:10.1007/BF00351550
21. M. Peiteado, J.F. Fernández, A.C. Caballero, J. Eur. Ceram. Soc **27**, 3867 (2007) doi:10.1016/j.jeurceramsoc.2007.02.046
22. L. Hozer, *Semiconductor Ceramics: Grain Boundary Effects* (Polish Scientific Publisher, Warszawa, 1973), p. 44
23. G.C. Miles, A.R. West, J. Am. Ceram. Soc **89**, 1042 (2006) doi:10.1111/j.1551-2916.2005.00799.x
24. M. Peiteado, M.A. De la Rubia, J.F. Fernández, A.C. Caballero, J. Mater. Sci **41**, 2319 (2006) doi:10.1007/s10853-006-7168-5